Published in final edited form as:
Inorg Chem. 2013 September 16; 52(18): . doi:10.1021/ic401563f.

Self-Organization of Zr(IV) Porphyrinoids on Graphene Oxide Surfaces by Axial Metal Coordination

Matthew Jurow[a], **Viacheslav Manichev**[a,‡], **Cesar Pabon**[a,‡], **Brian Hageman**[a], **Yuliya Matolina**[a], and **Charles Michael Drain**[a,b,*]

[a]Department of Chemistry and Biochemistry, Hunter College of the City University of New York

[b]Rockefeller University, 1230 York Avenue, New York, New York 10065 USA

Abstract

The protruding oxophilic central metal ion of Zr^{IV} porphyrinoids facilitates axial coordination to the oxygen bearing functional groups on graphene oxide (GO) surfaces to result in new supramolecular photonic materials with high dye loading especially on edges and large defects. The reaction proceeds at room temperature with GO dispersed in tetrahydrofuran and GO films on glass. Since the Zr^{IV} serves as a conduit, the photophysical properties of the dye sensitized GO derive from both the axially bound chromophores and the GO substrate. Self-organization of metalloporphyrinoids on GO mediated by axial coordination of group (IV) metal ions allows for direct sensitization of graphene and graphenic materials without requiring covalent chemistries with poorly conducting linkers.

Keywords

Graphene oxide; self-organization; zirconium; porphyrin and phthalocyanine; coordination chemistry

Introduction

The unique properties of graphene oxide (GO) have driven research on using GO in functional materials for diverse applications.[1–4] GO is produced by a variety of scalable methods that result in similar, but not identical, products.[5] Theories about the exact structure of GO have continuously evolved because of the non-homogenous nature of the material.[6] A commonly accepted model (Lerf-Klinowski) describes a surface composed of a substituted network of sp^2 and sp^3 hybridized carbon atoms. Alcohol and epoxide functionalities are present on the basal planes with carboxylic groups along the edges and larger defect sites of the flakes, which range between tens of nanometers and tens of microns in edge length and 0.8–1.5 nm in thickness if fully exfoliated depending on the method of production.[7]

Interest in GO has focused on properties arising from its non-stoichiometric nature resulting in regions of variable oxygen content, controllable dispersibility in water and organic

*Corresponding Author: cdrain@hunter.cuny.edu, 212-650-3791.
‡These authors contributed equally.

Author Contributions
The manuscript was written through contributions of all authors. All authors have given approval to the final version of the manuscript.

Supporting Information. AFM, TEM, optical spectroscopy, control studies with Zn dyes, electronic measurements. This material is available free of charge via the Internet at http://pubs.acs.org.

solvents,[8] interesting photonic properties,[9] and potential for use in biological systems such as for photodynamic therapeutics and for drug delivery.[1,10–14] Recent reports demonstrate GO applications in nonlinear optics,[15] as *p* or *n* type materials,[16,17] as a functional surfactant,[18] as antennae complexes to collect solar energy, and as efficient catalysts.[19]

Free base and metallotetraphenylporphyrins can be covalently bound to GO via amides[20,21] and esters,[22,23] or deposited by molecular beam[24] to yield photonic materials. Cationic porphyrins electrostatically associate with GO and rGO, and GO can be appended with polyethylene glycols to make biocompatible materials.[10,11] Large, planar phthalocyanines and their metalo derivatives associate with graphene and areas in reduced graphene oxide (rGO) via π-π interactions.[25–27] Sensitized hybrid GO materials can serve as components of solar cell devices,[28–30] and electrodes.[31]

We report herein the efficient self-organization and photonic properties of materials composed of 5,10,15,20-tetraphenylporphyrinato Zr^{IV}, Zr^{IV}(TPP), or phthalocyaninato Zr^{IV}, Zr^{IV}(Pc) (Figure 1) on graphene oxide, GO. The 7–8 coordinate oxophillic Zr^{IV} ions protrude from one face of the Zr^{IV}(TPP) and the Zr^{IV}(Pc) so that they are available to strongly coordinate to the bidentate acetates or oxygen containing functional groups or on the surfaces and edges of GO. The supramolecular material is assembled from dyes with acetates as auxiliary ligands, $Zr^{IV}(TPP)Ac_2$ and $Zr(Pc)Ac_2$, which are easily synthesized in good yields from commercially available precursors and have electronic spectra typical of metalloporphyrins and metallophthalocyanines, respectively.[32,33] The large ionic radius of Zr^{IV}, 0.72 Å, results in an unusual 0.9 Å to 1 Å displacement from the mean plane of the macrocycle nitrogen atoms, thereby enabling group IV metalloporphryrinoids to simultaneously bind oxygen groups on materials such as defects in polyoxometalates and to TiO_2 surfaces used in dye sensitized solar cells.[33–35] In contrast, Zn^{II} resides in the mean plane of the Pc and TPP macrocycles and is weakly six coordinate, thus Zn(TPP) and Zn(Pc) (Figure 1) do not strongly interact with GO and are used as control dyes for comparison of the photonic properties of the dye-sensitized GO materials.

Direct attachment of the chromophore to the GO surface via the protruding metal ion results in a coplanar orientation of the chromophores relative to the GO surface and at an angle on the edges and large defects. Some plausible geometries derived from MM2 calculations are suggested in Figure 2, and are consistant with Zr^{IV}(TPP) and Zr^{IV}(Pc) bound to a defect site in a polyoxometalate.[33] In contrast to covalent chemistry, this supramolecular chemistry approach increases the efficiency of dye loading, strongly couples the electronic properties of the two components, and preserves the properties of the substrate. The Zr^{IV} serves as a direct conduit for electronic coupling of the dye and GO systems because of the mixing of the metal ion and chromophore orbitals.[15,36] The photonic properties of this new hybrid material can be tuned by altering the photophysical properties of the dye, and represents an avenue for the development of a variety of sensitized graphenic materials.

Materials and methods

Atomic Force Microscopy (AFM) measurements were conducted with an Asylum Research Corp. (MFP-3D) or an Agilent 5500 instrument using standard n-type silicon cantilevers with reflective aluminum coating (MikroMasch NSC15-AlBS) with a nominal spring constant of 40 N/m and frequency of 325 kHz, at a scan rate of 15 μm/sec. UV-visible absorption spectroscopy was performed on a Cary 1-Bio UV-Visible spectrometer. Steady state fluorescence spectra were obtained on a HORIBA Jobin-Yvon FluoroLog-3 fluorometer. Quartz or optical glass cuvettes were used for all spectroscopic studies. All photophysical studies were carried out in distilled solvents. MM2 calculations were done in

Chem3D. Experiments have been repeated multiple times by at least three different researchers.

Zn(Pc) is synthesized by simple click-type substitution of peripheral fluorine atoms on the commercially available perfluorophthalocyanine precursor with thioalkanes to improve solubility.[37] Synthetic details of Zr^{IV} dyes are reported.[33] GO material was purchased from Graphene Supermarket who reports that the material is >60% single layer, flakes are 0.5–5 microns, and with 20% oxygen (w/w).

Optical Spectra

A dispersion of 0.1 mg/mL GO is made by sonicating single layer GO flakes in freshly distilled THF,[38] and titrated in 40 μL aliquots into 3 mL solutions of 3 μM $Zr^{IV}(Pc)Ac_2$ or 2 μM $Zr^{IV}(TPP)Ac_2$ in THF. After 24 h to allow the dyes to bind the GO, the UV-visible and fluorescence emission spectra were recorded in 1x1 cm cuvettes (λ_{ex}: 655 nm for Zn(Pc), 633 nm for $Zr^{IV}(Pc)$, 422 nm for Zn(TPP), and 417 nm for $Zr^{IV}(TPP)$). Fluorescence quenching comparisons were recorded at consistent absorbance values.

Nanocomposites

GO was added to 100 μM solutions of $Zr^{IV}(Pc)Ac_2$ or $Zr^{IV}(TPP)Ac_2$ in THF to make a 0.1 mg/mL GO solution, and sonicated for 5 min. to ensure good dispersion. After allowing 48 h for equilibration at room temperature, samples were centrifuged at 13,000 RPM for 15 min. and washed twice with fresh THF to remove unbound dye molecules.

AFM

Samples for AFM were prepared either by dip coating ozone cleaned glass into the suspensions of the nanocomposites in THF or by centrifuging the suspension, dispersing the pellet into nanopure water by sonication, and spin coating onto ozone cleaned glass.

TEM

All data were collected at 200 kV on a Jeol 2100 transmission electron microscope equipped with EDAX at the eucentric point to ensure reproducibility of the measurements. An 8 μL drop of the above nanocomposite dispersion was placed on a 300 mesh carbon coated copper grid (TED Pella Inc.) and allowed to dry for 1 min. before imaging.

Films

GO in aqueous suspension (3 mg/mL) was spin coated onto piranha cleaned quartz slides and dried in an oven to make 15 nm thick continuous films. Films were then soaked in 0.1 mM solutions of dyes in CH_2Cl_2 for three days at room temperature in the dark to ensure equilibration. The films were rinsed extensively with clean CH_2Cl_2 to remove any unbound dye and the backs of the slides were cleaned repeatedly with MeOH before spectra were recorded.

Probe Measurements

Devices were made by spin coating layers of GO (of 8 nm or 15 nm) onto ozone cleaned glass from an aqueous suspension. Sheet resistance was measured by Van der Pauw technique of the pristine GO layers, of an 8 nm GO film soaked in $Zr^{IV}(Pc)$ or $Zr^{IV}(TPP)$ (0.1 mM in CH_2Cl_2), or of an 8 nm GO film spin coated on top of a ca. 40 nm thick layer of $Zr^{IV}(TPP)$ or $Zr^{IV}(Pc)$ spin cast from chlorobenzene on ozone cleaned glass. Measurements were taken in the dark and under illumination.

Results and Discussion

GO dispersions in THF were added to solutions of $Zr^{IV}(Pc)Ac_2$ or $Zr^{IV}(TPP)Ac_2$ and allowed to react for 24 h to allow the maximal amount of the Zr^{IV}(Pc) or Zr^{IV}(TPP) to bind to GO. These are similar conditions used to bind the Zr^{IV} metalloporphyrinoids to surface oxygens on nanoparticles of TiO_2.[34] The UV-visible spectral shifts and decreased intensity in the Zr^{IV}(Pc) Q band (676 nm) and Zr^{IV}(TPP) Soret (421 nm) after incubation are consistent with displacement of the acetate ligands by the oxygen functional groups on the GO and formation of the hybrid material (Figure 3).[34] The intensity of the UV-visible spectra of the hybrid materials with Zr^{IV}(Pc) or Zr^{IV}(TPP) attached to GO monotonically decreases without changes in peak λ_{max} as the solution is diluted, thus indicating that the solution is homogeneously dissolved and the zirconium dyes are strongly bound to the GO. Since the zinc species, Zn(Pc) and Zn(TPP), cannot accommodate further ligation and do not chemically bond GO, the electronic spectra are not altered upon addition of the GO dispersion.

Significant fluorescence quenching of the Zr^{IV} dyes indicates charge injection from the chromophore excited state (HOMO −5.4 eV, LUMO −3.6 eV, band gap 1.8 eV)[34] into the GO made possible by the large band gap of GO (ca. −5.6 eV – −4.0 eV).[20,39–41] When binding is complete, the emission is quenched by 70% for the Zr^{IV}(Pc) and 30% for the Zr^{IV}(TPP), respectively. The quenching is consistent with electron transfer to the GO as found with covalently bound porphryinoids to graphene and GO.[4] Note that the peripheral phenyl groups on TPP are nominally orthogonal to the macrocycle with dihedral angles 90±20°, thus the phenyl moieties on Zr^{IV}(TPP) likely reduce binding to the surfaces of GO by steric hindrance. For Zn(TPP) and Zn(Pc) controls, the electronic absorption and emission spectra are unchanged by addition of the GO dispersion, indicating no interaction. Note that the large Stokes shift for the Zr^{IV}(Pc) is typical for these compounds.

To investigate the properties of the material in the solid state, films of GO were spin cast onto quartz substrates from dispersions in water, soaked in 0.1 mM dye solutions in CH_2Cl_2 for 72 h, and rinsed thoroughly with clean solvent. An aqueous GO dispersion of 3 mg/mL yielded 15 nm thick continuous films while a 1 mg/mL dispersion yielded an 8 nm film. After soaking in solutions of the $ZrTPP(ac)_2$ or $ZrPc(ac)_2$ and rinsing well with fresh THF, fluorescence quenching by charge transfer from Zr containing dyes to GO is observed for these metal-coordinated films (Figure 4).[42] UV-visible spectra demonstrate the presence of the coordinated dyes on the GO films by the absorbance from the Zr^{IV}(TPP) Soret (421 nm) and Zr^{IV}(Pc) Q (693 nm) bands (Figure 4). The small peaks from the control Zn^{II} complexes are likely the result of dye molecules interacting with the GO in graphene like regions through π-π interactions.

The absence of significant shifts in the optical spectra indicates that the dye molecules are not aggregated. Optical data on the films suggests a surface density[43] of ca. one chromophore per 20–50 nm^2, assuming average flakes of 1 μm^2 and dyes bound to only one face. The C:Zr mole ratio obtained by elemental analysis (31:0.006) of the Zr^{IV}(TPP) and Zr^{IV}(Pc) bound to GO indicated similar packing densities of ca. one per 40 nm^2. Collectively, these data indicate that the high oxygen content of the GO facilitates tight binding and high surface coverage of the Zr^{IV} dyes mediated by axial coordination.

In a separate experiment, $Zr^{IV}(Pc)Ac_2$ was added to a 0.1 mg/mL GO dispersion in THF to make solutions 100 μM in dye and ensure saturation of the GO surfaces with Zr^{IV} chromophores. Suspensions were allowed to react ca. 72 h to reach equilibrium, whereupon the mixture was centrifuged, rinsed with clean THF to remove unbound dye, and dispersed again in THF by brief sonication to form nanocomposites of GO with Zr^{IV}(Pc) coordinated

NIH-PA Author Manuscript
NIH-PA Author Manuscript

to the protruding oxygen containing surface and edge groups. Ozone cleaned glass slides were dip coated into these dispersions and rinsed well with clean THF. AFM analyses of these composite films confirm that the large oxygen:carbon ratio of the GO allows for high surface density of the coordinatively bound chromophores. Sonication in THF selectively removes dye molecules coordinated on the basal plane of the GO while preserving those coordinated more strongly to the flake edges, where there is a great concentration of carboxylic groups[44] (Figure 5). A single flake of GO is ca. 1.2 nm thick (Figure S8, S9),[45,46] and single layer flakes of GO coated on both sides with Zr^{IV}(Pc) are observed, corresponding to heights of ca. 2.8 nm. The total heights of the Zr^{IV}(Pc)/GO composite correspond well to those predicted by adding the heights of the GO with the thickness of the dye obtained from crystal structures (Figure 5, S10).[33] The AFM of control samples prepared by identical methods using Zn(Pc) and Zn(TPP) show GO ca. 1.1 nm flakes, and the absence of the zinc dyes.

TEM images of the same nanocomposites indicate a uniform coating of the GO surface with Zr^{IV}(Pc) and EDAX spectra display characteristic bands for the presence of Zr (Figure 6, S7). No evidence of Zn is observed by EDAX when GO is mixed with Zn(Pc) under the same conditions.

When the Zr^{IV}(Pc)/GO nanocomposites were centrifuged and redispersed in water, the nanocomposites precipitate rapidly, whereas the unfunctionalized GO remains suspended. This indicates a significantly increased hydrophobicity of the hybrid material relative to GO arising from the organic dye covering the face, and the lack of exposed oxygen species. Similar results are observed for the Zr^{IV}(TPP) on GO. To assess the robustness of the Zr^{IV} dye binding to the GO, the composite was sonicated (60 W, 30 minutes), and the solution was spin cast onto ozone cleaned glass coverslips. AFM of films of these samples display perforations of the graphene flakes resultant from removal of the oxophilic Zr^{IV}(Pc) or Zr^{IV}(TPP) (Figure S11). The perforation/degradation of the GO sheets also eliminates the fluorescence of the pristine GO flakes and no fluorescence was observed for the dyes.[9,47] Control experiments with Zn(Pc) and GO displays the characteristic UV-visible spectrum and broad fluorescence of GO without perforations. In a separate control experiment GO dispersions in THF were reacted with $ZrCl_4$. Large aggregates of metal ion cross-linked or intercalated GO sheets precipitate immediately. When dispersed by sonication into water no perforation or changes to the flakes are observed.

Four point probe measurements (Table S1) yielded sheet resistance values of 2.9×10^{10} and 3.6×10^{9} Ω/□ for 8 nm and 15 nm thick GO films, respectively.[48] For composite films, made by spin casting the Zr^{IV}(dye) treated GO or dipping the cast GO into Zr^{IV}(Pc) or Zr^{IV}(TPP) solutions, the sheet resistance of 8 nm films decreased by ca. 50%. This indicates the Zr^{IV} dyes can bridge some of the defects in the GO material, thereby increasing conductivity. Future work will investigate the properties of the dye/substrate interface as well as anticipated doping and photoconductivity applications.[8,16,49,50]

Layer-by-layer assembly is a simple technique to create functional materials with controlled size, morphology, and physical properties on different substrates.[51] Films were made by sequential dipping of quartz slides with an 8 nm GO layer into solutions of Zn(Pc), Zr^{IV}(Pc) or $ZrCl_4$ (Figure 7, Figures S13–16). Initially, the hydroxyl groups on the GO flakes associate with the quartz substrate, likely by hydrogen bonding.[52] The nonstoichiometric nature, oxidative debris, and varied size of the GO flakes result in imperfections and varied coverage in the initial layer, but these are filled in as the films develop in thickness. Zn(Pc) adheres to any hydrophobic basal plane regions of unoxidized sp^2 hybridized carbon allowing for layer growth mediated by the GO, but with small amounts of the dye entrained within the layers. Zr^{IV}(Pc) and $ZrCl_4$ both coordinate to the oxygenated regions of the GO.[8]

Binding of the chromophores and the addition of new layers of GO is indicated by the linear increase absorbance from the dyes and GO in the UV-visible spectra of the films. (Figure S15). Though individual layers are incomplete, sequential dipping of the substrate into the GO and Zr^{IV} dye solutions builds nanofilms with controlled thickness, controlled optical density, and controlled coverage. As observed in dye-coated GO dispersions, binding of the Zr^{IV} dyes to the GO significantly diminishes the propensity of the GO to interact and results in only a gradual increase in film thickness as the substrate is sequentially dipped in the solutions. We observed that the bound dye molecules also serve as nucleation points for the formation of microcrystals of dye, suggesting that GO might serve as a good substrate to grow microcrystals of other species. The highly varied composition of the GO affords many possible binding modes and binding sites for the Zr^{IV} dyes, for interactions between flakes of the GO, and for interactions with the substrate. The hydrophobic Zn dyes can interact with graphene like areas of the GO, while the oxophilic metal center can interact with oxygen functional groups on the GO and with the substrate.

Conclusions

Self-organization of a composite film of Zr^{IV} porphyrins or Zr^{IV} phthalocyanines on GO is accomplished by the concomitant coordination of the metal ion to both the dye and the carboxylate groups decorating the edges of the GO sheets and the OH groups on the planar surfaces of GO. This supramolecular approach affords a material with high surface coverage of the dyes on the GO substrate and better electronic coupling of the two systems compared to porphyrinoid attached to GO by covalent chemistry. The hybrid material displays photonic properties derived from both the dyes and the GO.[12] Reduced GO has enhanced electronic properties and the Zr^{IV} dyes should bind to remaining oxygen containing defect sites.[53] This type of direct sensitization will broaden the applications of GO and foster the creation of new composite functional materials using cost effective components and self-organization to create functional films.[54–58] These studies also indicate that the GO may serve as a means to grow microcrystals of other species.

Supplementary Material

Refer to Web version on PubMed Central for supplementary material.

Acknowledgments

Funding Sources

Supported by the U.S. National Science Foundation (NSF) CHE-0847997 and 1213962 to CMD. Hunter College science infrastructure is supported by the NSF, the National the National Institute on Minority Health and Health Disparities (8G12 MD007599) from the National Institutes of Health, and the City University of New York.

We thank Jacopo Samson for his work with TEM and EDAX spectra, Ivana Radivojevic for the Zr^{IV} dyes, and David Nissenbaum for help with figures.

ABBREVIATIONS

GO	graphene oxide
TPP	5,10,15,20-tetraphenylporphyrin
Pc	phthalocyanine
TEM	transmission electron microscopy
AFM	atomic force microscopy

References

1. Loh KP, Bao Q, Eda G, Chhowalla M. Nat Chem. 2010; 2:1015–1024. [PubMed: 21107364]
2. Chen D, Feng H, Li J. Chem Rev. 2012; 112:6027–6053. [PubMed: 22889102]
3. Wan X, Huang Y, Chen Y. Acc Chem Res. 2012; 45:598–607. [PubMed: 22280410]
4. Georgakilas V, Otyepka M, Bourlinos AB, Chandra V, Kim N, Kemp KC, Hobza P, Zboril R, Kim KS. Chem Rev. 2012; 112:6156–6214. [PubMed: 23009634]
5. (a) Dreyer DR, Park S, Bielawski CW, Ruoff RS. Chem Soc Rev. 2010; 39:228–240. [PubMed: 20023850] (b) Park S, Ruoff RS. Nature Nanotech. 2009; 4:217–224.
6. Rourke JP, Pandey PA, Moore JJ, Bates M, Kinloch IA, Young RJ, Wilson NR. Angew Chem Int Ed. 2011; 50:3173–3177.
7. Lerf A, He H, Forster M, Klinowski J. J Phys Chem B. 1998; 102:4477–4482.
8. Kim J, Cote LJ, Kim F, Yuan W, Shull KR, Huang J. J Am Chem Soc. 2010; 132:8180–8186. [PubMed: 20527938]
9. Melucci M, Durso M, Zambianchi M, Treossi E, Xia ZY, Manet I, Giambastiani G, Ortolani L, Morandi V, De Angelis F, Palermo V. J Mat Chem. 2012; 22:18237–18243.
10. Liu Z, Robinson JT, Sun X, Dai H. J Am Chem Soc. 2008; 130:10876–10877. [PubMed: 18661992]
11. Sun X, Liu Z, Welsher K, Robinson J, Goodwin A, Zaric S, Dai H. Nano Res. 2008; 1:203–212. [PubMed: 20216934]
12. Luo Z, Vora PM, Mele EJ, Johnson ATC, Kikkawa JM. Appl Phys Let. 2009; 94:111909.
13. Shih CJ, Lin S, Sharma R, Strano MS, Blankschtein D. Langmuir. 2011; 28:235–241. [PubMed: 22039913]
14. Yang Y, Zhang YM, Chen Y, Zhao D, Chen JT, Liu Y. Chem Eur J. 2012; 18:4208–4215. [PubMed: 22374621]
15. Yao C, Yan LK, Guan W, Liu CG, Song P, Su ZM. Dalton Trans. 2010; 39:7645–7649. [PubMed: 20401364]
16. Arnold MS, Zimmerman JD, Renshaw CK, Xu X, Lunt RR, Austin CM, Forrest SR. Nano Let. 2009; 9:3354–3358. [PubMed: 19637853]
17. Tung VC, Huang JH, Tevis I, Kim F, Kim J, Chu CW, Stupp SI, Huang J. J Am Chem Soc. 2011; 133:4940–4947. [PubMed: 21391674]
18. Tung VC, Kim J, Cote LJ, Huang J. J Am Chem Soc. 2011; 133:9262–9265. [PubMed: 21615169]
19. Yan JM, Wang ZL, Wang HL, Jiang Q. J Mat Chem. 2012; 22:10990–10993.
20. Xu Y, Liu Z, Zhang X, Wang Y, Tian J, Huang Y, Ma Y, Zhang X, Chen Y. Adv Mater. 2009; 21:1275–1279.
21. Karousis N, Sandanayaka ASD, Hasobe T, Economopoulos SP, Sarantopoulou E, Tagmatarchis N. J Mat Chem. 2011; 21:109–117.
22. Bala Murali Krishna M, Venkatramaiah N, Venkatesan R, Narayana Rao D. J Mat Chem. 2012; 22:3059–3068.
23. Melucci M, Treossi E, Ortolani L, Giambastiani G, Morandi V, Klar P, Casiraghi C, Samori P, Palermo V. J Mat Chem. 2010; 20:9052–9060.
24. Pandey PA, Rochford LA, Keeble DS, Rourke JP, Jones TS, Beanland R, Wilson NR. Chem Mat. 2012; 24:1365–1370.
25. Chunder A, Pal T, Khondaker SI, Zhai L. J Phys Chem C. 2010; 114:15129–15135.
26. Malig J, Jux N, Kiessling D, Cid JJ, Vázquez P, Torres T, Guldi DM. Angew Chem Int Ed. 2011; 50:3561–3565.
27. (a) Cárdenas-Jirón GI, Leon-Plata P, Cortes-Arriagada D, Seminario JMJ. Phys Chem C. 2011; 115:16052–16062.(b) Zhang XF, Xi Q. Carbon. 2011; 49:3842–3850.
28. Wang X, Zhi L, Mullen K. Nano Let. 2007; 8:323–327. [PubMed: 18069877]
29. Zhong S, Zhong JQ, Mao HY, Wang R, Wang Y, Qi DC, Loh KP, Wee ATS, Chen ZK, Chen W. ACS Appl Mater Interfaces. 2012; 4:3134–3140.

30. Park H, Howden RM, Barr MC, Bulović V, Gleason K, Kong J. ACS Nano. 2012; 6:6370–6377. [PubMed: 22724887]
31. Poursaberi T, Hassanisadi M. J Porphyrins Phthalocyanines. 2012; 16:1140–1147.
32. Brand H, Arnold J. Coord Chem Rev. 1995; 140:137–168.
33. (a) Falber A, Burton-Pye BP, Radivojevic I, Todaro L, Saleh R, Francesconi LC, Drain CM. Eur J Inorg Chem. 2009; 2009:2459–2466. [PubMed: 20543903] (b) Radivojevic I, Burton-Pye BP, Saleh RR, Ithisuphalap K, Francesconi LC, Drain CM. RSC Adv. 2013; 3:2174–2177.
34. Radivojevic I, Bazzan G, Burton-Pye BP, Ithisuphalap K, Saleh R, Durstock MF, Francesconi LC, Drain CM. J Phys Chem C. 2012; 116:15867–15877.
35. Radivojevic I, Burton-Pye BP, Saleh R, Ithisuphalap K, Francesconi LC, Drain CM. RSC Adv. 2013; 3:2174–2177.
36. Liao MS, Scheiner S. J Chem Phys. 2002:117.
37. Varotto A, Nam C-Y, Radivojevic I, Tomé PCJ, Cavaleiro JAS, Black CT, Drain CM. J Am Chem Soc. 2010; 132:2552–2554. [PubMed: 20136126]
38. Paredes JI, Villar-Rodil S, Martínez-Alonso A, Tascón JMD. Langmuir. 2008; 24:10560–10564. [PubMed: 18759411]
39. Zhang L, Xia J, Zhao Q, Liu L, Zhang Z. Small. 2010; 6:537–544. [PubMed: 20033930]
40. Yamaguchi H, Murakami K, Eda G, Fujita T, Guan P, Wang W, Gong C, Boisse J, Miller S, Acik M, Cho K, Chabal YJ, Chen M, Wakaya F, Takai M, Chhowalla M. ACS Nano. 2011; 5:4945–4952. [PubMed: 21618992]
41. Zhu Y, Li X, Cai Q, Sun Z, Casillas G, Jose-Yacaman M, Verduzco R, Tour JM. J Am Chem Soc. 2012; 134:11774–11780. [PubMed: 22716929]
42. Treossi E, Melucci M, Liscio A, Gazzano M, Samorì P, Palermo V. J Am Chem Soc. 2009; 131:15576–15577. [PubMed: 19824679]
43. Bazzan G, Smith W, Francesconi LC, Drain CM. Langmuir. 2008; 24:3244–3249. [PubMed: 18321141]
44. Quintana M, Montellano A, del Rio Castillo AE, Tendeloo GV, Bittencourt C, Prato M. Chem Com. 2011; 47:9330–9332.
45. Becerril HA, Mao J, Liu Z, Stoltenberg RM, Bao Z, Chen Y. ACS Nano. 2008; 2:463–470. [PubMed: 19206571]
46. Li D, Muller MB, Gilje S, Kaner RB, Wallace GG. Nat Nano. 2008; 3:101–105.
47. Thomas HR, Valles C, Young RJ, Kinloch IA, Wilson NR, Rourke JP. J Mat Chem C. 2013; 1:338–342.
48. Eda G, Fanchini G, Chhowalla M. Nat Nanotech. 2008; 3:270–274.
49. Jin M, Jeong HK, Yu WJ, Bae DJ, Kang BR, Lee YH. J Phys D: Appl Phys. 2009; 42:135109.
50. Chang C-H, Fan X, Li L-J, Kuo J-L. J Phys Chem C. 2012
51. Kovtyukhova NI, Ollivier PJ, Martin BR, Mallouk TE, Chizhik SA, Buzaneva EV, Gorchinskiy AD. Chem Mater. 1999; 11:771–778.
52. Zhao X, Zhang Q, Hao Y, Li Y, Fang Y, Chen D. Macromolecules. 2010; 43:9411–9416.
53. Luo D, Zhang G, Liu J, Sun X. J Phys Chem C. 2011; 115:11327–11335.
54. Beletskaya I, Tyurin VS, Tsivadze AY, Guilard R, Stern C. Chem Rev. 2009; 109:1659–1713. [PubMed: 19301872]
55. Drain CM, Varotto A, Radivojevic I. Chem Rev. 2009; 109:1630–1658. [PubMed: 19253946]
56. Radivojevic I, Varotto A, Farley C, Drain CM. Energy Environm Sci. 2010; 3:1897–1909.
57. Drain CM, Bazzan G, Milic T, Vinodu M, Goeltz JC. Israel J Chem. 2005; 45:255–269.
58. Jurow MJ, Hageman BA, DiMasi E, Nam CY, Pabon C, Black CT, Drain CM. J Mater Chem A. 2013; 1:1557–1565.

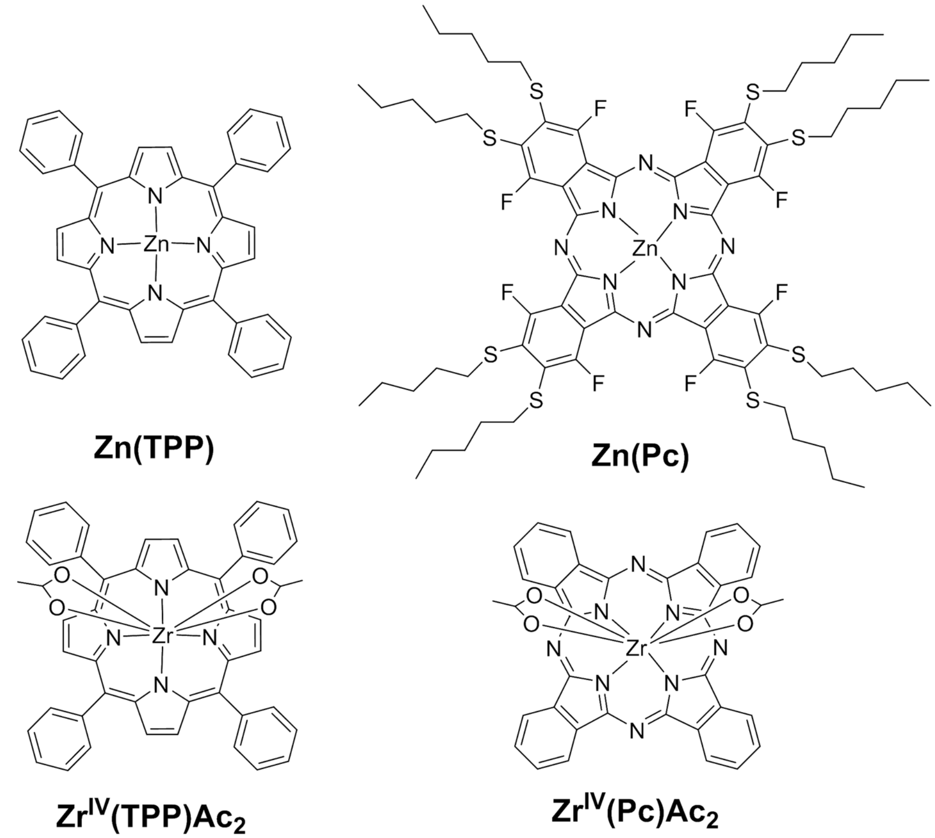

Figure 1.
Since the 8-coordinate Zr^{IV} ion protrudes from one face of the *5,10,15,20*-tetraphenylporphyrin (TPP) and phthalocyanine (Pc) the Zr^{IV} axially coordinates GO by replacement of bidentate acetate groups with oxygen groups on the GO (bottom). The 4-coordinate Zn analogue very weakly accepts axial ligands and does not bind GO (top).

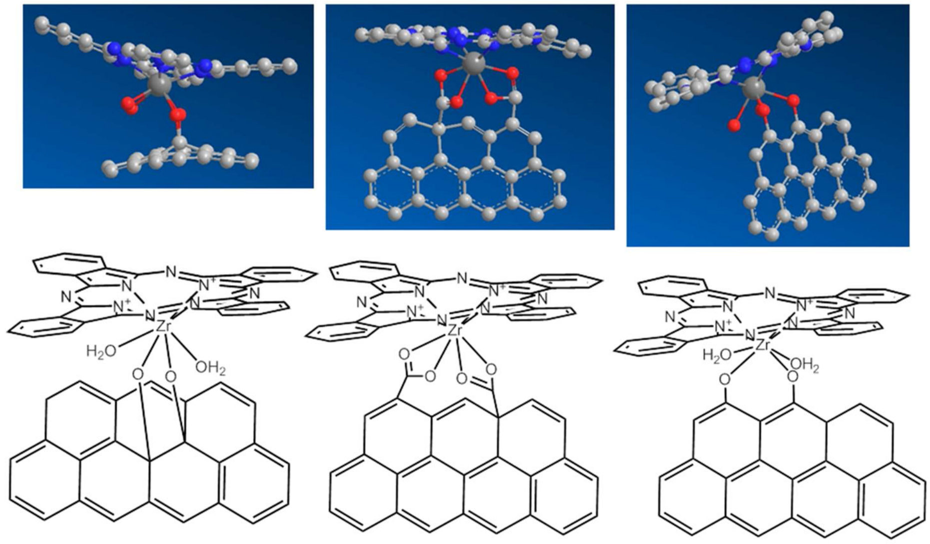

Figure 2.
Three ways of binding of Zr^{IV}(Pc) on a small region of GO are representative of the several possible binding modes The Zr^{IV}(TPP) bind similarly. 3-dimensional renderings are approximated from MM2 calculations (top, left to right) for internal diol, side carboxylates, and side diols; grey=C, blue=N, red=O, dark grey=Zr^{IV}, H left out for clarity.

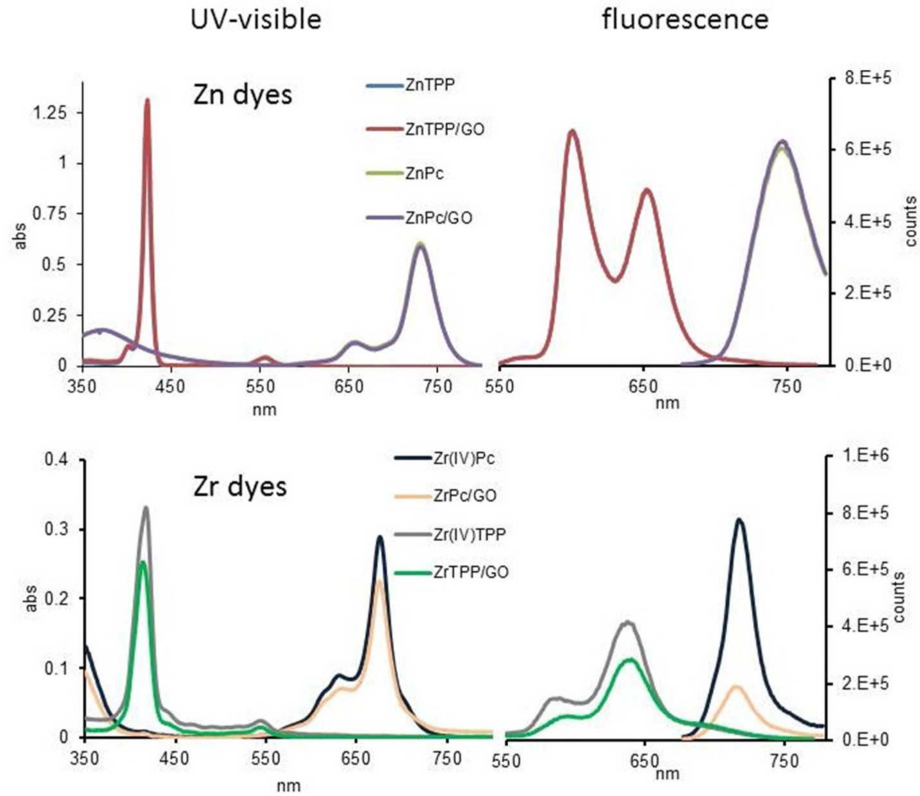

Figure 3.

Top: the UV-visible and fluorescence spectra of the Zn dyes overlap with the spectra after addition of 120 μL of 0.1 mg/mL GO dispersed in THF; indicating that neither ZnPc nor ZnTPP interact with GO. Bottom: the significant changes in the UV-visible and fluorescence quenching of $Zr^{IV}(TPP)Ac_2$ and $Zr^{IV}(Pc)Ac_2$ after addition of 120 μL of 0.1 mg/mL GO dispersed in THF indicate exchange of the acetate ligands for oxygen functional groups on the GO and binding of the metalo dyes. λ_{ex} = 417 nm for Zr^{IV}(TPP) and Zn(TPP), λ_{ex} = 633 nm for Zn(Pc) and Zr^{IV}(Pc), in each case the optical density was <0.1.

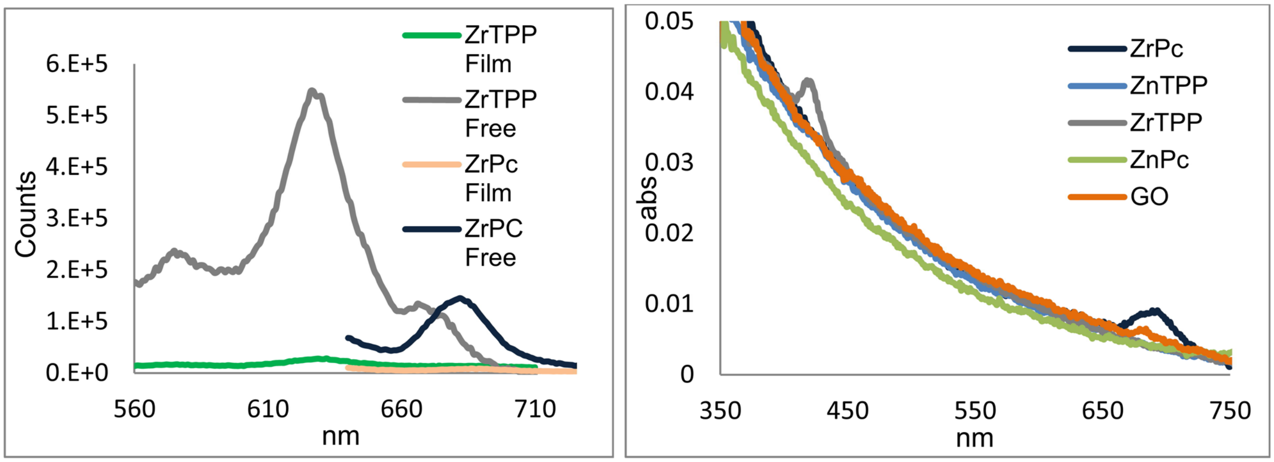

Figure 4.
Left: fluorescence of Zr^{IV}(Pc) and Zr^{IV}(TPP) dyes bound to a ca. 15 nm thick film of GO quenched compared to solutions of the unbound dyes with the same optical density. λ_{ex} = 417 nm for Zr^{IV}(TPP) and 633 nm for Zr^{IV}(Pc). Right: UV-visible spectra of the same GO films where control Zn dyes are not observed to bind the GO films.

NIH-PA Author Manuscript
NIH-PA Author Manuscript

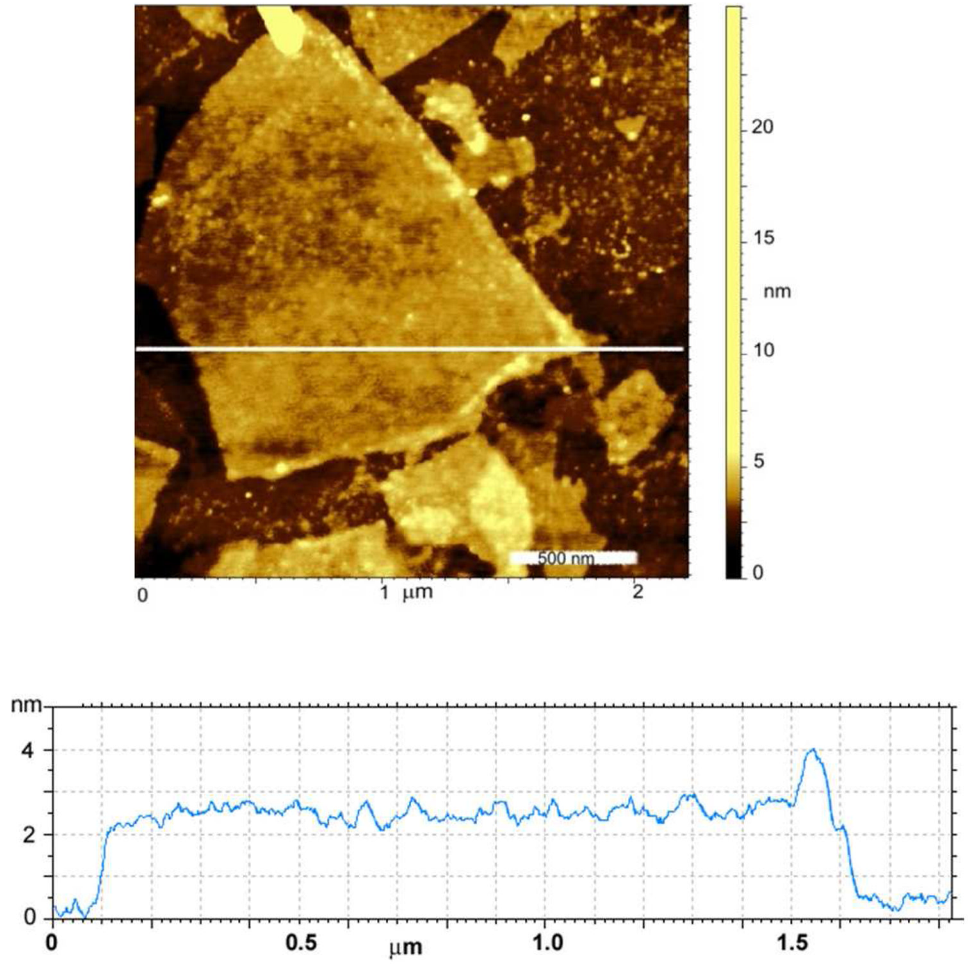

Figure 5.

AFM image and height trace of ca. 2.8 nm high GO flake coated on both sides with Zr^{IV}(Pc) cast onto an ozone cleaned glass coverslip. Higher dye loading on GO edge is visible.

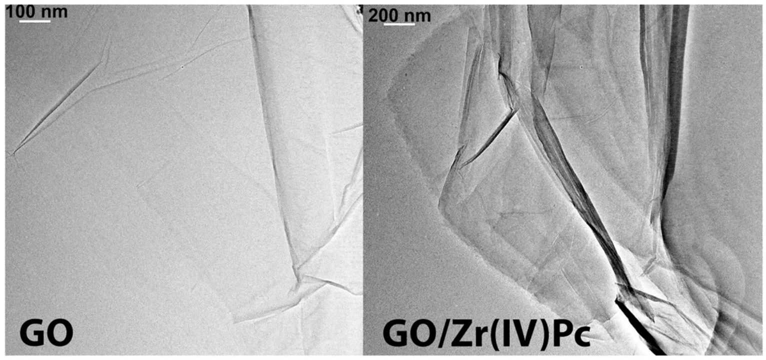

Figure 6.
TEM images of GO flakes treated with Zn(Pc) (left) or $Zr^{IV}(Pc)Ac_2$ (right) and rinsed with clean solvent. Full surface coverage by coordinated Zr^{IV} dye is indicated by EDAX spectra (see supporting information) and greater contrast, which also indicates greater dye loading on GO edge. The Zn dyes are completely removed by simple rinsing.

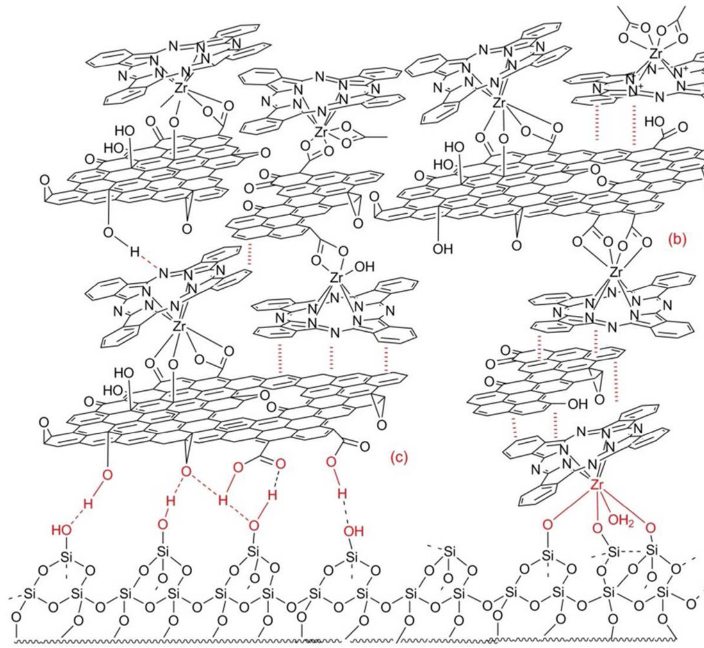

Figure 7.

Representation of the possible intermolecular interactions between in multilayers of dye-bound GO made by layer-by-layer methods. Interactions between the GO and Zr^{IV}(Pc) with the quartz substrate include: (a) π-π interactions between the starting $Zr^{IV}(Pc)Ac_2$, (b) coordination of the protruding Zr^{IV} ion of the Pc to the oxygen groups on GO, (c) H-bonds between the substrate and the GO. The higher density of oxygen groups at the edges of GO result in greater binding of the Zr^{IV} dyes, see Figure 5. Other variations of these interactions are also present, e.g. H-bond and π-π interactions between GO flakes, see Figure S13.